

Impact of Irrigation Area on Cloud Appearance around the Yellow River in China

Hiroaki Kawase¹, Takao Yoshikane¹, Masayuki Hara¹, Shingo Ohsawa², and Fujio Kimura^{1,3}

1. Frontier Research Center for Global Change, Yokohama, Japan

2. Weathernews Corporation, Chiba, Japan

3. Graduate School of Life and Environmental Sciences, University of Tsukuba, Tsukuba, Japan

1. Introduction

The Hetao irrigation district is located in the western part of Inner Mongolia, China (Fig. 1). The elevation is about 1000m above sea level. The district is situated in a semi-arid zone, where the annual total precipitation is about 200mm. The cultivated land is 0.514 million ha, 93 % of which is irrigated by the Yellow River. Five billion m³/year water from the Yellow river is expended in the area (Oeu et al., 2005). Satellite observation shows a difference in the surface condition between the irrigation area and the surrounding area. During the daytime in summer, the statistics of satellite images indicate that the frequency of cloud appearance over the area is lower than the cloud appearance over the surrounding area (Sato et al., 2007, submitted).

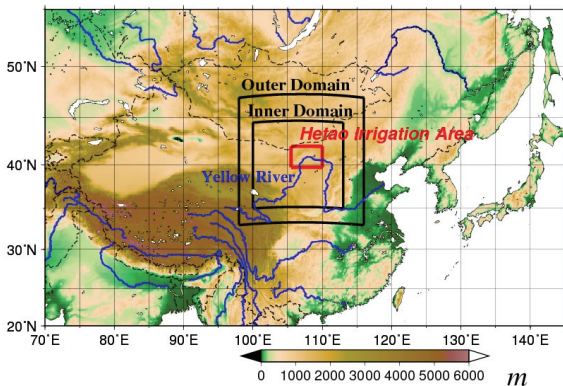


Figure 1. Geophysical map of East Asia. The outer and inner domains in the numerical experiments are shown as black solid-lined boxes.

Figure 2 shows three true color satellite snapshots at 13:30 Local Time (LT) on 3 August 2005, 14:10 LT on 4 August 2005, and 13:15 LT on 5 August 2005. They are obtained by the MODIS/Aqua. No clouds appear over the Hetao irrigation district located at the center of the figure. The district is surrounded by mountains and hills, so the suppression of clouds can be explained by thermally-induced local circulations between mountains and a plain. However, a relationship between convection and a surface condition has been pointed out by many studies (Clark and Arritt, 1995; Emori, 1998; Pielke, 2001). An abundance of soil moisture and active

vegetation on the irrigation area may also contribute to suppressing the clouds. The purpose of this study is to reveal the role of the irrigation in the suppression of cloud using a numerical model.

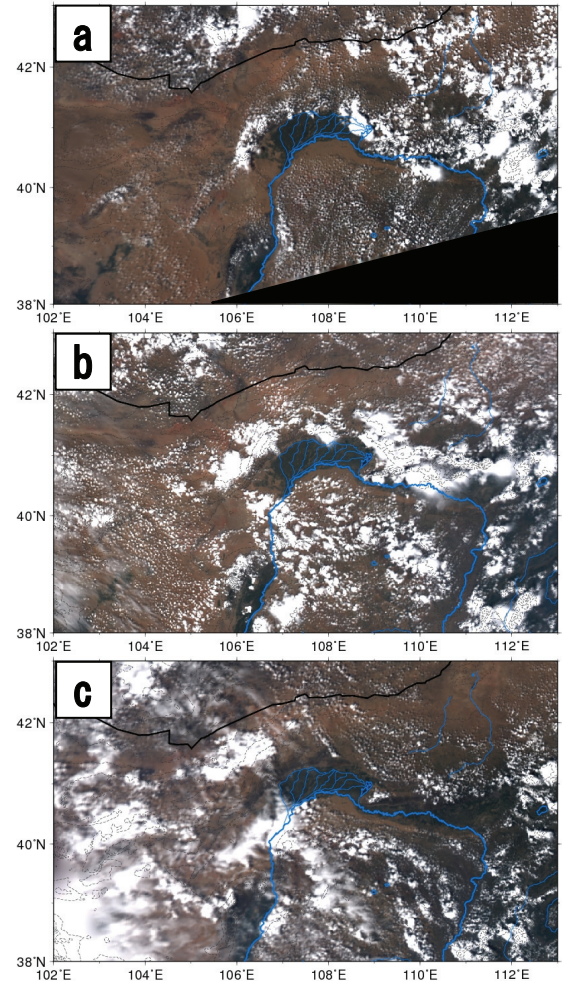


Figure 2. True color images observed by MODIS/Aqua at (a) 13:30 LT on 3 August 2005, (b) 14:10 LT on 4 August 2005, and (c) 13:15 LT on 5 August 2005.

2. Satellite data and numerical experiments

2.1 Satellite date

A true color image and a land surface temperature are obtained by MODIS/Aqua. The former is provided by the Level 1 and Atmosphere Archive and Distribution System (LAADS) of the Goddard Space Flight Center, NOAA, and the latter is provided by Land Processes Distributed Active Archive Center (LPDAAC) which is a part

of NASA's Earth Observing System (EOS) Data and Information System (EOSDIS), respectively.

2.2 Specification of numerical experiments

Numerical experiments are conducted using a non-hydrostatic numerical model, Advanced Research Weather Research and Forecasting (WRF) modeling system Version 2.2. Two-way nested grid systems are adopted. The coarse grid system and the fine grid system have grid intervals of 15km and 3km, respectively. The domains of this simulation are shown as two black solid-line boxes in Fig. 1. WRF Single Moment 6-class graupel microphysics scheme is used in both domains. Land surface, surface-layer and boundary-layer processes are represented by the Noah land surface model, the Monin-Obukhov (Janjic Eta) scheme, and the Mellor-Yamada-Janjic (Eta) TKE scheme, respectively. The initial and lateral boundary conditions for the coarse grid system are interpolated from the 6-hourly NCEP global tropospheric analyses data (1x1 degree grids, 24 vertical levels). The simulations were executed from 00 UTC 1 August.

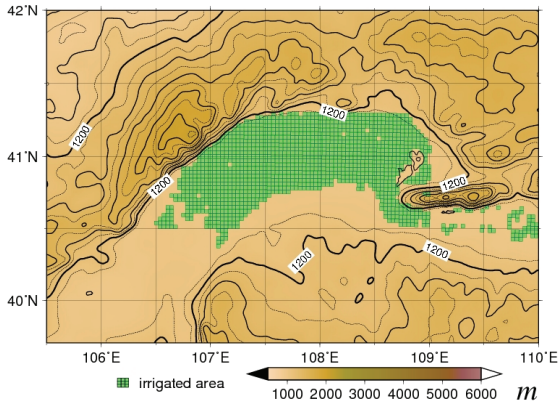


Figure 3. Analysis domain. Green area is assumed as a virtual irrigation area, where soil moisture is different in each numerical experiment.

| Volumetric Soil Water Content | 0.1 | variation | 0.2 |
|-------------------------------|---------|-----------|------------|
| RUN NAME | SWC-0.1 | SWC-VAR | SWC-0.2 |
| Volumetric Soil Water Content | 0.3 | 0.4 | saturation |
| RUN NAME | SWC-0.3 | SWC-0.4 | SWC-SAT |

Table 1. Specification of numerical experiments

We assume a virtual irrigation area (hereafter V-irrigation area), which is based on the satellite image, in the model (see the green area in Figure 3). Six numerical experiments were conducted

using different amounts of soil moisture in the V-irrigation area. Fluctuating volumetric soil water contents are used in the V-irrigation area in the SWC-VAR, while fixed volumetric soil water contents are used in the other five experiments (Table 1). Volumetric soil water content is fluctuating except for the V-irrigation area in all experiments (Figure 4).

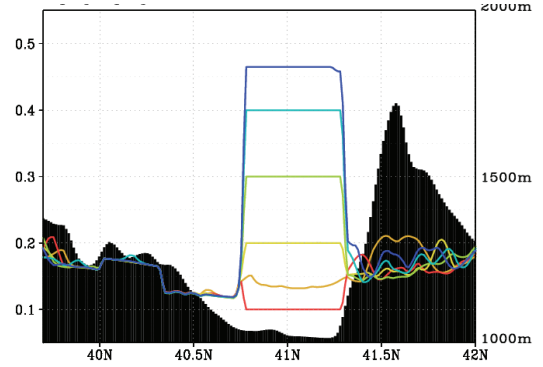


Figure 4. Topography and volumetric soil water content along 108E in each experiment at 13LT in 3 August 2005.

3. Difference of Cloud Appearance depending on amount of soil moisture

We focus the days from 3 August 2005 to 5 August 2005 when a suppression of the cloud is remarkable over the Hetao irrigation district (see Fig. 1). Figure 5 shows land surface temperature observed by MODIS/Aqua at 13:30 in 3 August 2005. A clear thermal contrast is observed between the Hetao irrigated area and the surrounding area.

Figure 6 shows a distribution of the vertical integrated solid and liquid cloud water simulated by the SWC-0.3 and SWC-VAR at 14LT in 3 August 2005. In the SWC-0.3, a lot clouds appear over the northern mountains and a southern hill, while little clouds appear over the center of the V-irrigation area (Fig. 6a). The result is quite similar to Fig. 2a. On the other hand, a lot of clouds appear not only over the mountains and the hill but also over the V-irrigation area in the SWC-VAR (Fig. 6b). The other experiments using a moist (dry) surface condition results in the decrease (increase) of clouds in the V-irrigation area (figure not shown). Similar cloud distribution appears in the other two days.

Figure 7 shows a diurnal cycle of a percentage of clouds appearing over the V-irrigation area during the three days (from 3 to 5 in August). In all experiments, the percentages begin to increase after 10 LT, which achieves the maximum around

13 LT. Cloud appears most frequently in the SWC-0.1. The SWC-VAR is next to the SWC-0.1. The other experiments show low frequencies of the cloud appearance. Some experiments show a second peak around 18 LT, which results from transportsations of clouds which are generated over the north mountains in August 3. Figure 7 denotes that the moist land surface suppresses the generation of cloud particularly in the early afternoon.

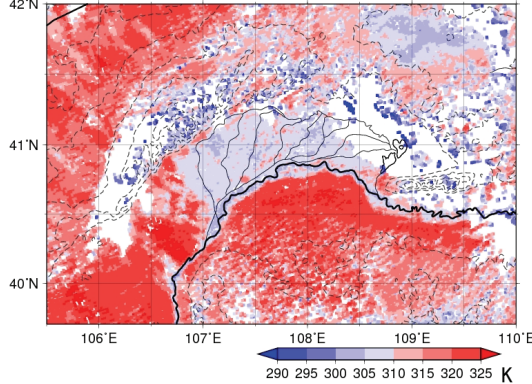


Figure 5. Land surface temperature observed by MODIS/Aqua at 13:30 in 3 August 2005.

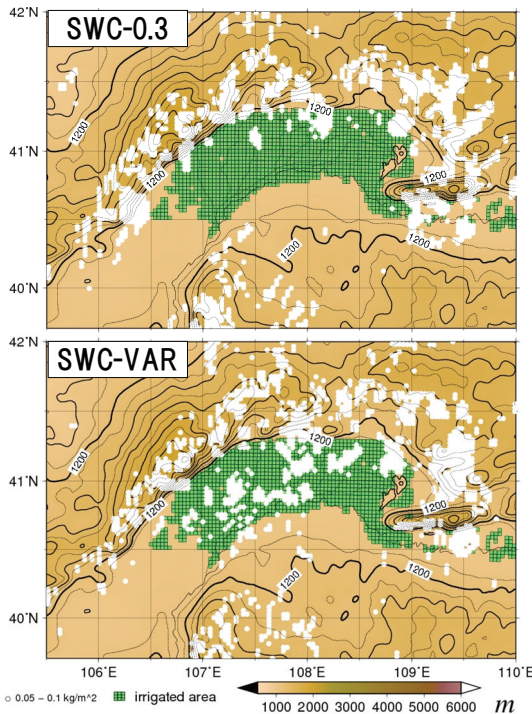


Figure 6. Distribution of the vertical integrated solid and liquid cloud water simulated by the SWC-0.3 (upper panel) and SWC-VAR (lower panel) at 14LT on 3 August 2005.

The high land surface temperature, which is as same as that on the southern area, is calculated on the V-irrigation area in the SWC-0.1 and

SWC-VAR. The land surface temperature lowers as the soil moisture is increasing. As the results, the contrast of the land surface temperature becomes large between the V-irrigation area and the surrounding area similar to the observation (Fig. 4).

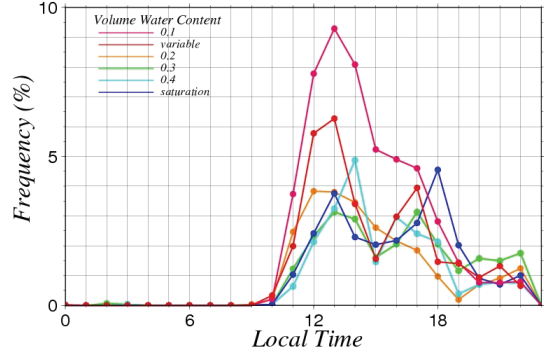


Figure 7. Diurnal cycle of percentages of cloud appearing over the V-irrigation area during the three days.

4. Mechanism of Suppression of Cloud over the Irrigated Area

Table 2 shows the mean sensible and latent heat flux from the V-irrigation area at 13 LT during the three days. Lower sensible heat flux is calculated in the experiments using moister land surface, which suggests that a shallow convection can not be developed over the moist land surface. On the other hand, latent heat flux is higher in the experiments. Bowen ratio is below 1.0 in the SWC-0.2, SWC-VAR, and SWC-0.1.

| RUN NAME | SWC-0.1 | SWC-VAR | SWC-0.2 |
|-----------------------|---------|---------|---------|
| SH (W/m^2) | 476.6 | 400.5 | 324.4 |
| LE (W/m^2) | 11.6 | 97 | 181.8 |
| Bowen Ratio | 0.02 | 0.24 | 0.56 |
| RUN NAME | SWC-0.3 | SWC-0.4 | SWC-SAT |
| SH (W/m^2) | 205.5 | 87.5 | 35.9 |
| LE (W/m^2) | 324.1 | 486.1 | 568.4 |
| Bowen Ratio | 1.58 | 5.56 | 15.83 |

Table 2. Mean sensible and latent heat flux over the V-irrigation area at 13 LT during the three days.

Figure 8 shows a vertical-latitude cross section of zonal mean vertical wind from 107.5E to 108.5E at 13 LT during the three days. Downward wind is predominant over the V-irrigation area, while upward wind is predominant over the northern mountain and the southern hill in the SWC-0.4. Downward wind also appears over some parts of the southern hill, which indicates a lot of active shallow convection. The PBL height over the

V-irrigation area is lower than that over the surrounding region (Fig. 8a). The compensating downward wind associated with the upward wind over the surrounding area also contributes to suppress the development of planetary boundary layer (PBL) and cloud generations over the V-irrigation area. The result of SWC-SAT is similar to figure 8a except for a stronger downward wind and a lower PBL height (figure not shown).

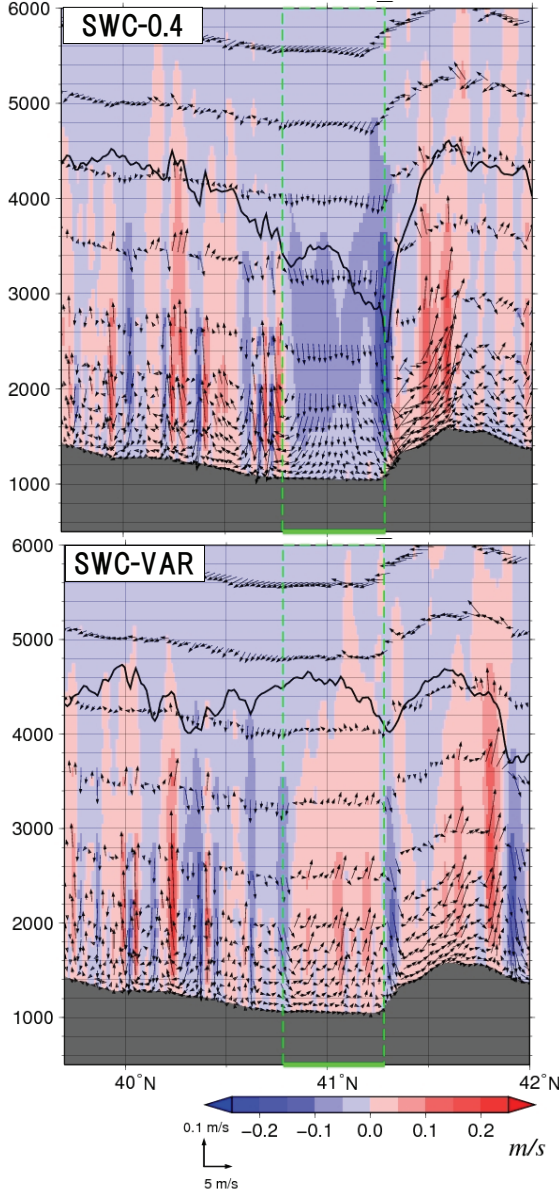


Figure 8. Vertical-latitude cross sections of zonal mean vertical wind and from 107.5E to 108.5E at 13 LT during the three days (from 3 to 5 August 2005) simulated by SWC-0.4 (upper panel) and SWC-VAR (lower panel). Green lined area means the V-irrigation area. Black line means a PBL height. A gray area means topography.

On the other hand, upward wind is predominant over the whole area in the SWC-VAR (Fig. 8b). The high PBL is calculated over the V-irrigation area as same as that over the surrounding area.

5. Conclusion

The impacts of the irrigation area on cloud appearance around are revealed using the satellite images and the numerical experiments. Numerical experiments indicate that cloud does not appear over the virtual irrigated area where high volumetric soil water content is applied, which is quite similar to the observation by MODIS/AQUA. On the other hand, a lot of cloud appears over the virtual irrigated area where dry surface condition is applied. The results suggest that the moister land-surface tends to suppress the clouds more strongly over the area. The small sensible heat flux from the moist irrigation area suppresses the development of a planetary boundary layer. The compensating downward wind associated with the upward wind over the surrounding dry area also contributes to suppress the cloud over the irrigation area. We conclude that the contrast of surface temperature depending on the amount of soil moisture can produce the difference of the cloud-appearance in addition to the local circulation between mountains and plains.

Acknowledgements

This research was supported by "Global Environment Research Fund by Ministry of Environment Japan" B-061.

References

- Clark, C. A., and P. W. Arritt, 1995: Numerical simulations of the effect of soil moisture and vegetation cover on the development of deep convection. *Mon. Wea. Rev.*, **34**, 2029–2045.
- Oeu, T., T. Tamoto, H. Ikawa, and K. Takase, 2005: Micrometeorological model for estimating Evapotranspiration from an irrigated maize field in the Hetao irrigation district in the Yellow River Basin. *J. Agric. Meteorol.*, **60**, 537-540.
- Pielke, R. A., 2001: Influence of the spatial distribution of vegetation and soils on the prediction of cumulus convective rainfall. *Reviews of Geophysics*, **39**, 151-177.
- Sato, T., F. Kimura, and A. Hasegawa, 2007: Vegetation and topographic control of cloud activity over arid/semiarid Asia, *J. Geophys. Res.*, submitted.
- Seita, E. 1998: The interaction of cumulus convection with soil moisture distribution: An idealized simulation. *J. Geophys. Res.*, **103**, 8873-8884.